RESEARCH ARTICLE

A Polyherbal Formulation Habb-e-Ustukhuddus Induces Apoptosis and Inhibits Cell Migration in Lung and Breast Cancer Cells without Any Toxicity in Mice

Reenu Punia[1], Mansoor Ali[1], Yasmeen Shamsi[2], Rana P. Singh[1,3]*

Abstract

Objective: A polyherbal medicine, Habb-e-Ustukhuddus (HU), is used for its anti-inflammatory properties. However, the anticancer and chemopreventive properties of HU were not known, and Therefore, investigated in the present study. **Methods:** Cancer cells were treated with 50-400 µg/ml HU and MTT, trypan blue, and clonogenic assays were performed. Propidium iodide (PI) staining, annexin V-FITC assay, and JC-1 staining were done for cell cycle progression, apoptosis, and mitochondrial membrane potential, respectively, using flow cytometry. Immunoblotting, cell migration and invasion assays were performed. Chemical characterization of HU was done through GC-MS and HPLC analyses. C57BL/6 mice were used to assess the *in vivo* toxicity of HU. **Results:** While evaluating the anticancer activity, the methanolic extract of HU (50-400 µg/ml) strongly inhibited the growth and survival ($P<0.05$-0.001) of lung and breast cancer cells and increased the cell population in the sub-G1 phase of the cell cycle. HU caused apoptotic death of cancer cells ($P<0.05$-0.001), which was associated with the depolarization of mitochondrial membrane potential ($\Delta\psi$) ($P<0.001$) and an increase in Bax to Bcl-2 protein ratio. Further, HU inhibited the invasion and migration of cancer cells, which was accompanied by an increase in the epithelial marker, E-cadherin, and a decrease in the mesenchymal marker, vimentin. The HU characterization by GC-MS and HPLC analyses showed the abundance of bioactive compounds including flavonoids and alkaloids. In the chemopreventive study, the oral administration of methanolic extract of the formulation HU (50 and 100 mg/kg body weight) to mice did not cause any toxicity and significantly increased the specific activities of hepatic drug metabolizing phase I and phase II enzymes, which suggested for its detoxification potential of xenobiotic compounds. **Conclusion:** Together, these results demonstrated the anticancer potential HU, without any apparent toxicity in mice, and thus HU could be further explored for its clinical utility in cancer control.

Keywords: Habb-e-Ustukhuddus (HU)- chemopreventive- hepatoprotective- anticancer.

Introduction

The cancer burden is growing rapidly in both developed and developing countries (Sung et al., 2021). Despite the advances in technology used for the diagnosis and treatment of cancer, it is still one of the leading causes of mortality around the globe (Miller et al., 2016). Although chemotherapy is common for cancer treatment, it is expensive and associated with adverse health effects, non-specificity, and chemoresistance. Cancer chemoprevention is an emerging discipline that utilizes natural, synthetic, or other biochemical agents to inhibit, delay and reverse the process of cancer development (Benetou et al., 2015; Buyel 2018). Ayurveda and Unani medicines use natural compounds which are cost-effective, relatively non-toxic, and easily available and thus could be a better alternative for cancer prevention and therapeutics.

The Unani system of medicine contains the knowledge of cancer disease from ancient times (Aslam et al., 1981). In the Unani system, the terminology for cancer is Sartan (an Arabic word), which is considered a disease of black bile (*Sawda*), and caused by excessive production and collection of black bile (Naaz 2017). Galen (129-199AD) was the first Unani physician who described most of the cancers and their management in Unani medicine (Uddin et al., 2015). Galen accepted Hippocrates' basic theory of cancer and classified it into three types (i) *Onkoi* (lumps or masses), (ii) *Karkinomas* (non-ulcerating), and (iii) *Karkinos* (malignant ulcers) (Alam et al., 2013). In the past few decades, several studies have been conducted to analyze the anticancer efficacies of medicinal plants used in Unani medicine. These plants include a satin (*Artemisia absinthium*) (Shafi et al., 2012), aftimun (*Cuscuta reflexa* Linn.) (Suresh et al., 2011), amla (*Emblica officinalis*

[1]Cancer Biology Laboratory, School of Life Sciences, Jawaharlal Nehru University, New Delhi, India. [2]Department of Moalajat, School of Unani Medical Education and Research, Jamia Hamdard, New Delhi, India. [3]Special Centre for Systems Medicine, Jawaharlal Nehru University, New Delhi, India. *For Correspondence: rana_singh@mail.jnu.ac.in

Gaertn.) (Zhao et al., 2015), asgand (*Withania somnifera* (L.) Dunal) (Rai et al., 2016; Sivasankarapillai et al., 2020), baladur (*Semecarpus anacardium* Linn.) (Nair et al., 2009), Gilo (*Tinospora cordifolia* (Thunb.) Miers) (Palmieri et al., 2019), Halela (*Terminalia chebula* Retz.) (Ravi Shankara et al., 2016), Kutki (*Picrorhiza kurroa)* (Soni and Grover, 2019) etc. However, the studies on Unani drugs for their anticancer activities are limited.

In the current study, we have investigated for the first time the effects of a classical polyherbal drug, Habb-e-Ustukhuddus (HU) on cancer cell growth, survival and migration, and associated changes at cellular and molecular levels. Further, chemical profiling of this drug was done to explore its phytochemical constituents. An *in vivo* mouse study was done to determine its toxicity and hepatomodulatory activity on Phase I and Phase II enzymes and antioxidant parameters.

Materials and Methods

Reagents and antibodies

Habb-e-Ustukhuddus (HU) was procured from Hamdard Laboratories, Ghaziabad, India. It was prepared as per the composition given in the National Formulary of Unani Medicine (NFUM, Part IV), and shown in Supplementary Table S1. All the reagents for HPLC and GC-MS analyses, and cell culture were purchased from Sigma Aldrich, USA. Primary antibodies for Bcl-2, #2872; Bax, #2772; E-cadherin, #14472; Vimentin, #5741; and Beta-actin, #A3853 and seconday antibodies, anti-mouse, #7076 and anti-rabbit, #7074P2 were procured from Cell Signaling Technology, USA.

Preparation of HU extract

The polyherbal formulation HU was dissolved in methanol (0.1 mg/ml) and kept at 37°C overnight at shaking. After 24 hours, the solution was sonicated for 30 minutes at 37°C and centrifuged at 5,000 rpm for 15 minutes. The supernatant was collected and kept in an oven at 40°C to evaporate the methanol. The remaining dried extract was collected and stored at 4°C for further use. The dried extract of HU was dissolved in double-distilled water for treating cells.

Cell culture

The human non-small cell lung cancer (NSCLC) cell lines, A549 and H1299, were purchased from NCCS Pune, India. Human prostate cancer cell lines, DU145 and PC-3 and epithelial human breast cancer cell line MDA-MB-231 were from ATCC, VA, USA. A549, H1299, and MDA-MB-231 cells were maintained in DMEM (Dulbecco modified Eagle's medium), while PC-3 and DU145 cells were grown in the RPMI-1640 medium. Both the mediums were supplemented with 10% fetal bovine serum (FBS) (Gibco Life Technology, USA) and PSA (Penicillin-Streptomycin-Amphotericin) antibiotic solution (Himedia, India). Cell culture was maintained at 37°C in humidified 5% CO2 incubator. Cells were allowed to grow as adherent monolayer and media was changed on alternative days. Cells were treated with the desired concentrations of HU dissolved in double-distilled water for desired time points.

MTT assay for cell viability

Cell viability was determined by using MTT assay. Cells (7.5×10^4 cells/well) were seeded in 96-well plates and incubated overnight at 37°C. Cells were treated with 100, 200, and 400 µg/ml concentrations of HU for 48 hours and then exposed to MTT {3-(4, 5- dimethylthiazol-2-yl)-2, 5-diphenyltetrazolium bromide} (Kumar et al., 2019). After 4 hours of incubation of cells with 100 µl/well of 0.5 mg/ml MTT at 37°C, media was aspirated from each well and 100 µl of DMSO was added to dissolve the formazan crystals formed by metabolically viable cells. The viability of the cells was measured by monitoring the absorbance at 570 nm by a microplate reader (Synergy H1 Hybrid Reader, BioTek, USA).

Trypan blue dye exclusion assay

The growth inhibitory and cell death effects of HU on cancer cells were determined by trypan blue dye exclusion assay as described earlier (Punia et al., 2017; Sabarwal et al., 2017). Briefly, 1×10^5 cells were seeded in 6-well plates and after 24 hours, cells were treated with 50-400 µg/ml concentrations of HU. After 48 hours of treatment, cells were harvested by trypsinization, stained with trypan blue dye, and counted for live and dead cells under a phase-contrast microscope.

Colony formation assay

Cells with density of 500 cells/well were seeded in a 6-well plate and treated with 50-100 µg/ml concentrations of HU after 24 hours of seeding. Cells were kept in the incubator for 7 days to form a colony. At the end of treatment, cells were washed, fixed, and stained with 0.05% crystal violet dye, and colonies were counted with phase contrast microscope.

Flow cytometric analysis for cell cycle phase distribution

A549 and MDA-MB-231 cells were seeded, treated, collected, and processed for cell cycle analysis as reported earlier (Kumar et al., 2019). Cells were resuspended in saponin/propidium iodide (PI) solution (0.3% saponin, 0.1% mM EDTA, 25 µg/ml PI, and 10 µg/ml RNAse) in PBS and kept at 4°C for 4 hours in dark condition. Cell cycle phase distribution was analysed by flow cytometry (FACS Aria III (BD Biosciences, USA).

Annexin V-FITC assay for apoptosis

Cells were seeded and treated as described for trypan blue assay. After 48 hours of treatment, cells were processed according to the manufacturer's protocol given with Annexin V-FITC apoptosis detection kit (BD Pharmingen, USA). The cells were analysed by flow cytometry (BD Biosciences, USA) to score annexin V and PI positive cells.

JC-1 staining for mitochondrial membrane potential

To determine the mitochondrial membrane potential cells were seeded and treated with HU as described in the trypan blue assay. The cell pellet was resuspended with 1 ml of fresh media containing 1.25 µl of JC-1 dye from 1

mg/ml dye stock and incubated in the dark for 15 minutes at 37℃. Cells were washed twice with 1× PBS and subsequently examined by flow cytometry to determine the ratio of JC-1 monomer/dimer.

Western immunoblot analysis

Cells (5×10^5 per 100-mm culture plate) were seeded and after 24 hours, treated with different concentrations of HU for 48 hours. The whole-cell lysate was prepared in nondenaturing lysis buffer and protein estimation was done by the Bradford method as published earlier (Shyanti et al., 2017; Kumar et al., 2019). Cell lysates were resolved on SDS-PAGE and proteins were transferred onto the PVDF membrane followed by blocking with 5% blocking buffer at room temperature. The membrane was incubated with a specific primary antibody followed by horseradish peroxidase–conjugated secondary antibodies and processed further for ECL detection. The band intensity on the film was quantified with ImageJ software (NIH, USA).

Wound healing assay

A549 and MDA-MB-231 cells were cultured in a 6-well plate and incubated at 37℃. When cell confluency reached around 95%, cells were pre-treated with 5 µg/ml mitomycin C for 3 hours to inhibit cell proliferation. A linear wound was made with a sterile micropipette tip by scratching the cell monolayer. Cells were washed with media to remove the floating cells and treated with 50-100 µg/ml of HU. The width of the wound was recorded by capturing the images at different time points using an inverted microscope.

Invasion assay

A549 cells were seeded and treated with 50-100 µg/ml of HU for 48 hours. Cells were collected followed by washing with serum-free media. A total of 40,000 live cells were seeded in the upper chamber of a Matrigel-coated transwell containing 500 µl serum-free media with HU. Cells were allowed to invade for 16 hours towards the lower chamber filled with media containing 10% FBS. Invaded cells at the bottom of the membrane were fixed, stained with crystal violet, and counted as described earlier (Rajput et al., 2021).

Gas chromatography and mass spectrum (GC-MS) analysis

GC-MS analysis was carried out at Advanced Instrumentation Research Facility (AIRF) at Jawaharlal Nehru University (JNU), New Delhi, India with GC-MS QP-2010 ultra-model. Helium was used as carrier gas with a constant flow of 1 ml/minute (split ratio = 10:0). The initial oven temperature was programmed from 50℃ and ended with 300℃ with 17 minutes of hold time. The injection temperature was 260℃, the ion source temperature was 220℃, the interface temperature was 270℃, and the solvent cut time was 4.50 minutes. The total GC run time was 45 minutes.

High-performance liquid chromatography (HPLC) analysis

The HPLC analysis of a methanolic extract of polyherbal formulation HU was done by using a C18 reverse-phase chromatography column. The gradient mobile phase was the mixture of 1% aqueous acetic acid (solvent A) and methanol (solvent B) in different proportions according to the gradient program as shown in Supplementary Table 2. Chromatographic separation of the compounds in the formulation was done at 278 nm wavelength using 20 µl injection volume and 1 ml/minute flow rate.

Animal study

Male C57BL/6 (6-8 weeks old) mice were obtained from Central Laboratory Animal Resources (CLAR), JNU, New Delhi for *in vivo* and *ex vivo* studies. Animals and protocol were approved by the Institutional Animal Ethics Committee, JNU, New Delhi, India. The mice were provided with standard food pellets and drinking water ad libitum and kept in a room with controlled temperature and humidity with 12 hours light/ 12 hours dark cycle at the CLAR facility. The animals were divided randomly into four groups (n = 6 mice/group) and orally administered with saline suspension of 50 and 100 mg of methanolic extract of HU/kg body weight of mouse on a daily basis for 15 days. Doxorubicin (5 mg/kg body weight of mouse) was used as positive control and given on the 1st, 6th, and 11th day of the treatment by intraperitoneal injection. Body weight, diet weight, and water consumption by mice were recorded on alternative days for any sign of toxicity.

After completion of the treatment mice were euthanized by CO_2 asphyxiation, and whole liver was immediately perfused with ice-cold saline and rinsed into 0.15 M Tris-KCl buffer (PH 7.4) on ice. The liver was weighed and 10% homogenate was prepared using 0.15 M Tris-KCl buffer. The homogenate was divided into two parts; 0.5 ml was used for measuring the level of acid-soluble sulfhydryl group (-SH), while the remaining was processed to isolate cytosolic and microsomal fractions as described earlier (Singh et al., 2000).

Biochemical analysis of tissue samples

Determination of serum glutamate pyruvate transaminase (SGPT) or alanine transaminase (ALT) and serum glutamate oxaloacetate transaminase (SGOT) or aspartate transaminase (AST) was done from mice blood serum according to the methods reported earlier (Sengupta et al., 2011). The microsomal peroxidative damage was estimated using the thiobarbituric acid reactive substances (TBARS) method (Varshney and Kale, 1990). Reduced glutathione (GSH) content was estimated as the total non-protein sulfhydryl group by the method described earlier (Singh et al., 2000). The activity of superoxide dismutase (SOD) was determined at 420 nm as per the method mentioned earlier (Marklund and Marklund, 1974). The specific activity of catalase was calculated as moles of H_2O_2 reduced/minute/mg protein at 240 nm (Aebi, 1984). Assays of NADPH-cytochrome P450 reductase and NADH-cytochrome b5 reductase were performed according to the method reported earlier

(Nauman et al., 2018). The specific activity of glutathione S-transferase (GST) in the cytosol was assayed by the method published earlier (Habig et al., 1974).

Statistical analysis

The results are presented as mean±SEM. Statistical analysis was done by using Graph Pad Prism software. Student's t-test was used for the significance of the difference between two groups and multiple comparison was done using one way ANOVA test. The value of P<0.05 was considered significant.

Results

HU inhibited growth and viability of human lung and breast cancer cells

To evaluate the anticancer potential of HU, MTT assay was performed using lung (A549, H1299), breast (MDA-MB-231), and prostate (DU145 and PC-3) cancer cell lines. We observed that 100-400 µg/ml of HU did not show considerable inhibition in growth and viability of H1299, DU145, and PC-3 cells (data not shown). However, HU decreased the cell viability of A549 cells by 40% (P < 0.001) after 48 hours of treatment (Figure 1A). HU caused dose-dependent inhibition of cell viability up to 50% (P < 0.001 to 0.01) in MDA-MB-231 cells after 48 hours of treatment (Figure 1B). We further assessed its anti-proliferative potential by using trypan blue dye exclusion assay in A549 cells. HU (50-400 µg/ml) decreased the total live cells by 7-71% (P < 0.001) (Figure 2A), and increased the dead cells by 29% (P < 0.001) at 400 µg/ml concentration (Figure 2B). It also inhibited the clonogenic potential of both A549 and MDA-MB-231 cells at 50-100 µg/ml concentration (Figure 2C and D). These results suggested that HU inhibits the proliferation and survival of lung and breast epithelial cancer cells. Therefore, for further studies, we used lung (A549) and breast (MDA-MB-231) cancer cells.

HU caused accumulation of cancer cells in sub-G1 phase of cell cycle

The cell cycle phase distribution was analysed to explore the growth inhibitory mechanisms of Unani formulation in cancer cells. We have observed a significant increase of 8% (P < 0.01) in the sub-G1 population of the cell cycle after treatment of 400 µg/ml of HU to A549 cells after 48 hours at the expense of G1 phase cell population (Figure 3A). In MDA-MB-231 cells, HU caused 7% and 70% (P < 0.05 to 0.001) increase in sub-G1 population at 200 µg/ml and 400 µg/ml concentrations, respectively (Figure 3B). These results suggested that HU increases sub-G1 cell population having less than 2N DNA content, and therefore, it may cause apoptosis in cancer cells which was studied next.

HU induced apoptosis in cancer cells

Since, there was an increase in dead cells as well as sub-G1 cell population by the treatment with HU, therefore, we performed annexin V-FITC analysis to assess apoptotic cell death in cancer cells. HU increased apoptotic cells by 3.5 fold (P < 0.001) and 18 fold (P < 0.001) at 200 and 400 µg/ml concentrations, respectively in A549 cells (Figure 4A and B). Similarly in MDA-MB-231 cells, HU caused up to 14 fold (P < 0.05) increase in the apoptotic cell population (Figure 4C and D).

We further measured the expression of apoptosis-associated mitochondrial proteins, Bax (pro-apoptotic) and Bcl-2 (anti-apoptotic). There was a strong increase in the expression of Bax (19-50 fold) and a decrease in the Bcl-2 (57-68%) protein levels after 48 hours of HU treatment of A549 cells (Figure 4E). HU strongly increased the Bax to Bcl-2 ratio, which is an indication of mitochondrial dysfunction and apoptosis induction (Figure 4E). Therefore, next we evaluated the effect of HU on mitochondrial membrane potential.

HU caused mitochondrial membrane depolarization in cancer cells

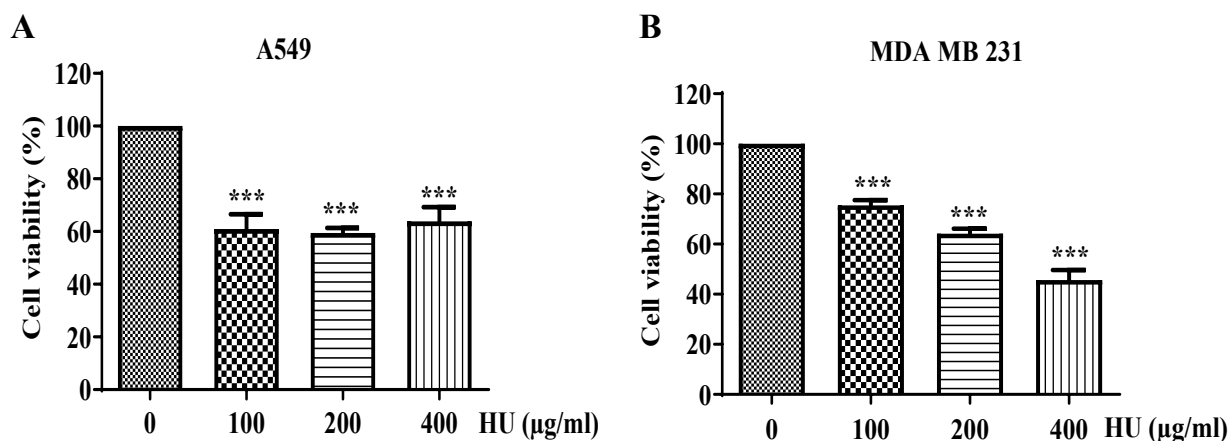The induction of apoptosis may be mediated through

Figure 1. Effects of HU on Cell Viability of Epithelial Cancer Cells. (A) A549 and (B) MDA-MB-231 cells were treated with different concentrations of HU for 48 hours and assessed for cell viability by MTT assay. Results are representative of three independent experiments. Data points are the means ± s.e.m. of three experiments. Bars, s.e.m, *P < 0.05, **P < 0.01, ***P < 0.001. HU, Habb-e-Ustukhuddus

A

B

C A549

Control   HU 50 µg/ml   HU 100 µg/ml

D MDA-MB-231

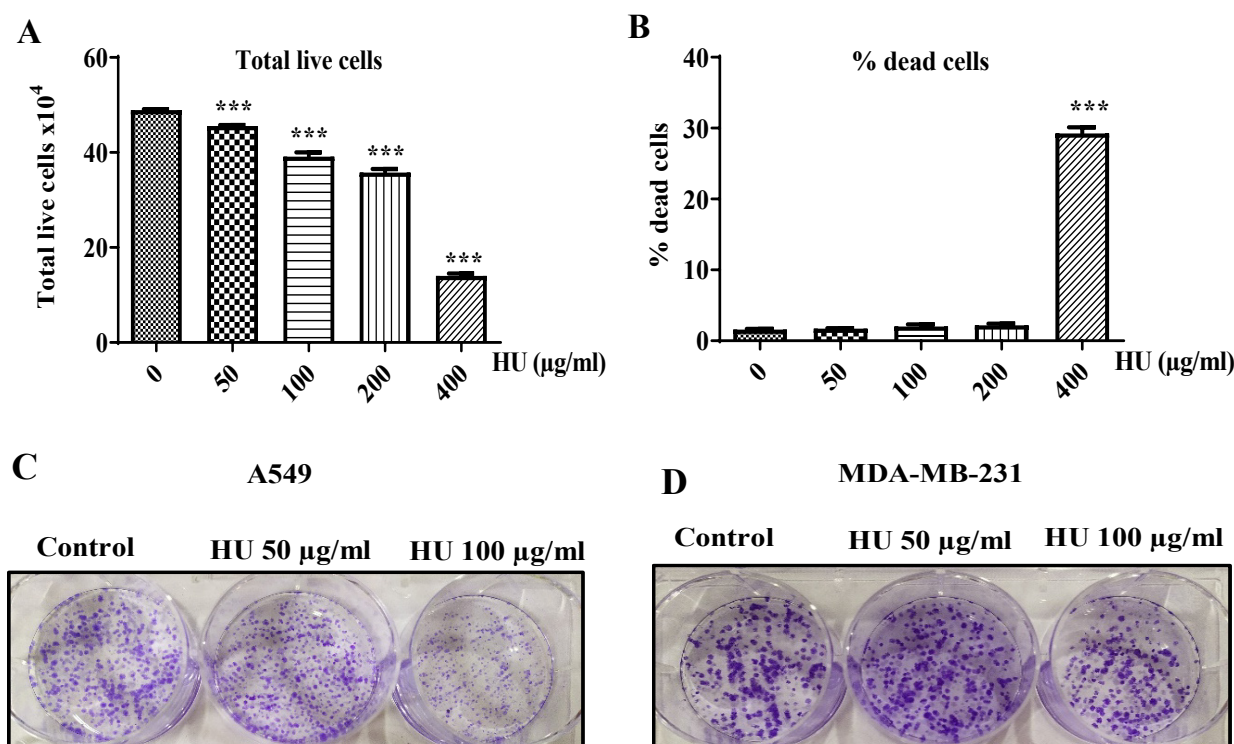Control   HU 50 µg/ml   HU 100 µg/ml

Figure 2. Effects of HU on Cell Proliferation and Clonogenicity of Cancer Cells. Effects of HU on A549 cell proliferation and death were measured by trypan blue assay, representing total live cells (A) and percent dead cells (B). The clonogenicity potential of cancer cells was assessed after the HU treatment to A549 and MDA-MB-231 cells in 6-well plates. Media was changed after every 3 days with respective treatments. On 8th day, cells were fixed and stained with crystal violet solution. (C) Images of A549 and (D) MDA-MB-231 colonies, respectively. Results are representative of three independent experiments. Data points are the means ± s.e.m. of three experiments. Bars, s.e.m, ***P < 0.001. HU, Habb-e-Ustukhuddus.

the loss or change in mitochondrial membrane potential, which can be analysed using JC-1 cationic dye. JC-1 forms dimer in the mitochondria of live cells, whereas in apoptotic cells, it comes out of mitochondria due to loss of mitochondrial membrane potential and dissociates into monomers (Singh et al., 2013). A549 cells showed dissociation of JC-1 dimer to monomer after 48 hours of HU treatment (Figure 5A). The monomer/dimer ratio was increased by upto 2-5 fold (P < 0.05-0.001) by the treatment with 200-400 µg/ml of HU (Figure 5B). These findings revealed that HU induced mitochondria-mediated apoptosis as a potential cell death mechanism in lung cancer cells.

HU suppressed migration and invasion of cancer cells

We assessed the effect of non-cytotoxic doses of HU on the migration potential of cancer cells. It was observed that 100 µg/ml of HU reduced the migration of A549 cells by 29% (P < 0.05),represented as the percentage of wound width, after 48 hours of treatment (Figure 6A and B). In MDA-MB-231 cells, HU (50-100 µg/ml) inhibited the cell migration by 32% (P < 0.01) at 12 hours (Figure 6C).

To further validate the results and anti-invasive potential of HU, we performed the transwell matrigel invasion and migration assay (Figure 7A). We found 25% (P < 0.001) and 58% (P < 0.001) inhibition on invasion and migration capacity of A549 cells after treatment with 50 and 100 µg/ml of HU, respectively (Figure 7B). At the molecular level, the expression of epithelial marker

E-cadherin was dose-dependently increased with 50 and 100 µg/ml of HU in A549 cells after 48 hours of treatment (Figure 7C). The mesenchymal marker, vimentin was decreased by up to 77% with HU treatment (Figure 7C). These results suggested that HU has strong inhibitory potential for invasion and migration of epithelial cancer cells.

Chemical profiling of methanolic extract of HU and identification of bioactive compounds

GC-MS technique combines gas-liquid chromatography and mass spectrometry (Kell et al., 2005), and it is a well-established method for profiling secondary metabolites present in plants as well as non-plant species (Fernie et al., 2004). Therefore, we performed GC-MS analysis of the methanolic extract of HU using NIST (National Institute Standard and Technology) standard library to identify the chemical constituents. A total of 72 compounds were detected (Figure 8A, left panel), out of which the most abundant ten compounds are shown in Figure 8A, right panel. GC-MS analysis revealed the presence of bioactive compounds such as eugenol, hexadecanoic acid and 9,12-octadecadienoyl chloride. To further identify and quantify the potential bioactive compounds, we used HPLC analysis, a known comprehensive analytical method for this purpose (Nag et al., 2020) (Figure 8B). The HPLC analysis showed that 100 mg/ml of HU contained epicatechin (1,472 µg/ml), salicin (1,174 µg/ml), gallic acid (677 µg/ml) and acetylsalicylic acid (633 µg/ml)
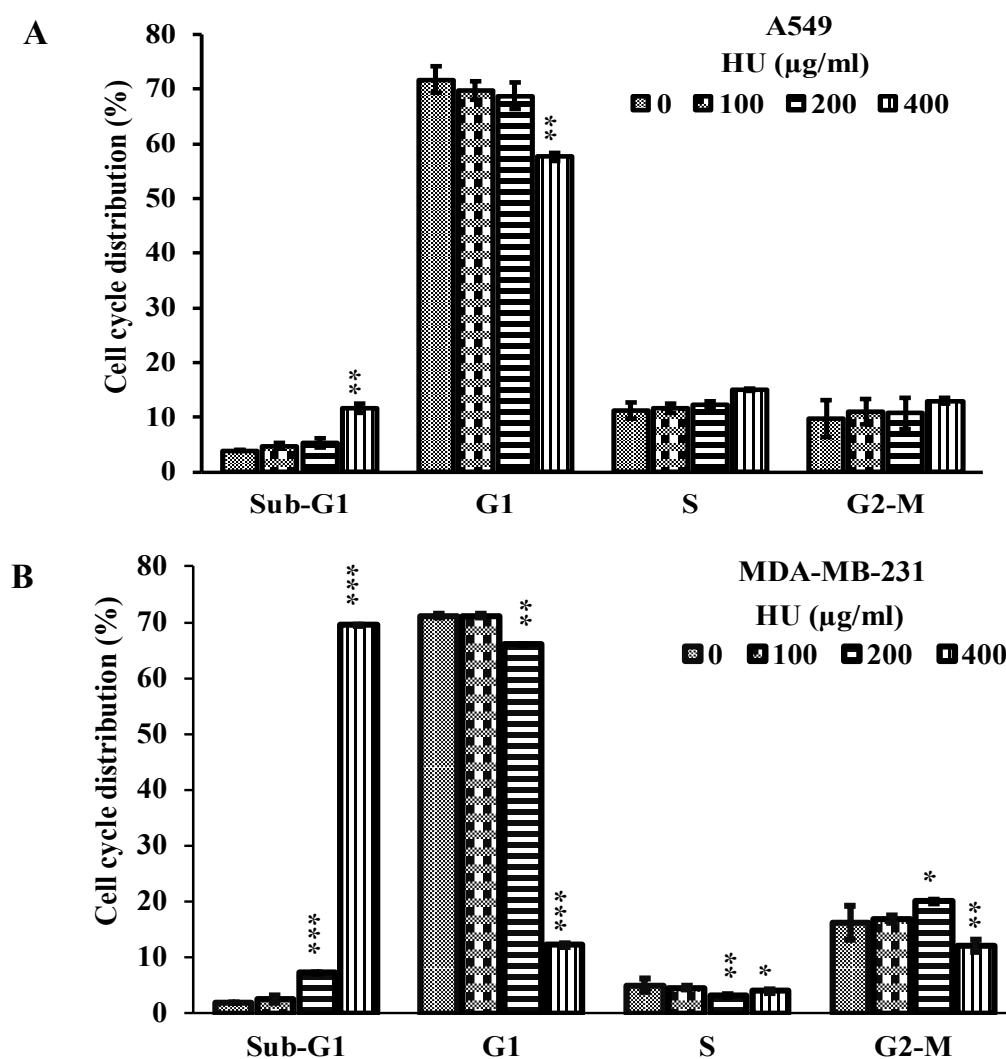
Figure 3. Effects of HU on Cell Cycle Progression of Cancer Cells. (A) A549 and (B) MDA-MB-231 cells were treated with HU and examined for different phases of the cell cycle as detailed in materials and methods. The bar graph represents the effect of HU treatment on cell cycle phases distribution. The data sets represent the mean ± s.e.m. from three independent experiments. Bars, s.e.m, *P < 0.01, **P < 0.01, ***P < 0.001. HU, Habb-e-Ustukhuddus.

in the highest concentrations (Figure 8B). Resveratrol (334.69 µg/ml) was another bioactive known anticancer compound found in the HU extract.

HU did not show any apparent toxicity in mice

Mice did not show any significant alteration in body weight gain, diet consumption, and water intake during 15 days of HU treatment with 50 and 100 mg/kg body weight given orally (Figure 9A, B, and C). Intraperitoneal injection of doxorubicin (5 mg/kg body weight on days 1, 6, and 11; total 3 doses) caused significant damage to the liver as observed by the significant increase in the levels of SGOT (AST) and SGPT (ALT) enzymes in mice serum (P < 0.05), however, HU did not show any significant effect on these enzymes (Figure 9D and E). Lipid peroxidation in the microsomal fraction of liver homogenate, measured by malondialdehyde (MDA) formation, was significantly increased with doxorubicin treatment (P < 0.05), whereas increasing doses of HU kept the level of MDA similar to control (Figure 9F). GSH, SOD, and catalase enzymes have an important role in the defense system of antioxidant enzymes. GSH is known to protect the cells

from oxidative damage and maintain redox homeostasis. GSH was significantly increased (P < 0.001 to 0.05) by HU treatment, whereas, doxorubicin decreased the level of GSH by 21-28% (P < 0.001) (Figure 9G). The specific activities of SOD were decreased by doxorubicin treatment whereas HU did not show any alterations (Figure 9H). The catalase activity though increased by both but was not found to be significant from the control (Figure 9I). Hence, HU did not have any adverse impact on antioxidant status in mice.

Phase I and II hepatic xenobiotic metabolizing enzymes

In phase I enzyme, cytochrome P450 reductase (cyt P450R) and cytochrome b5 reductase (cyt b5R) were assayed from the microsomal fraction of liver homogenate. Treatment of mice with 50 mg/kg and 100 mg/kg body of HU caused 2.4 and 2.6 fold increases (P <0.05 to 0.001) in specific activity of cyt P450R, respectively, however, the specific activity of cyt b5R remained unaltered (Figure 9J and K). The modulatory effect of HU on phase II hepatic enzyme glutathione S-transferase (GST) was assayed by using a cytosolic fraction of liver homogenate. HU
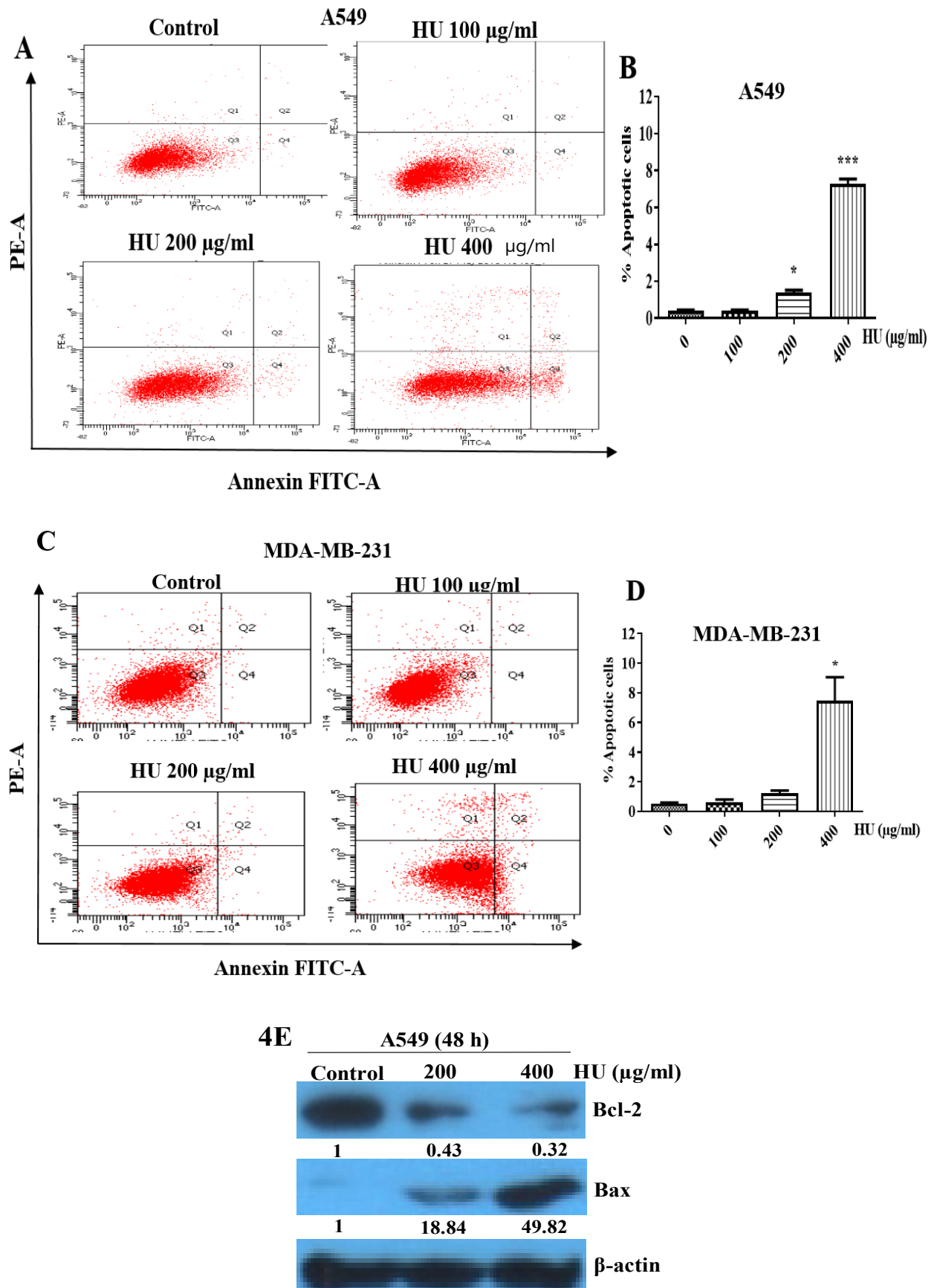
Figure 4. Effects of HU on Apoptosis in Cancer Cells. (A) A549 and (C) MDA-MB-231 cells were treated with respective doses of HU and stained with annexin V and PI followed by flow cytometry analysis for apoptotic cells. (B) & (D) the bar graphs show the percentage of apoptotic cell death of A549 and MDA-MB-231 cells, respectively. (E) A549 cells were treated with different concentrations of HU for 48 hours, and cell lysates were analysed for Bax and Bcl-2 proteins by western blotting. Results are representative of three independent experiments. Data points are the means ± s.e.m. of three experiments. Bars, s.e.m, *P < 0.05, ***P < 0.001. HU, Habb-e-Ustukhuddus.
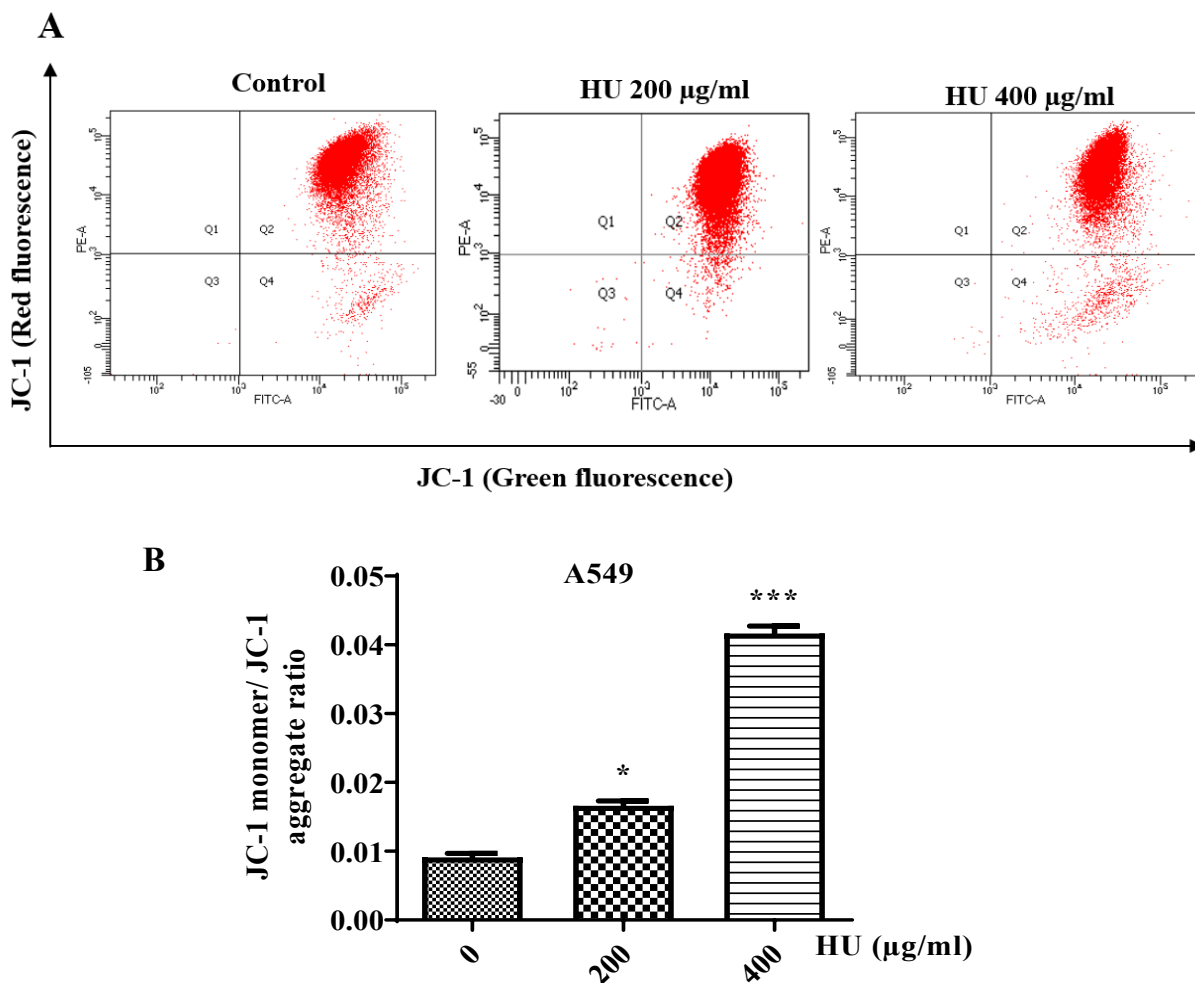
A

B

Figure 5. Effects of HU on Mitochondrial Membrane Potential of Cancer Cells. (A) A549 cells were treated with HU and its effect on the mitochondrial membrane potential of cells was examined after staining with JC-1 dye. (B) The bar graph represents the ratio of JC-1 monomer to dimer. Results are representative of three independent experiments. Data points are the means ± s.e.m. of three experiments. Bars, s.e.m, *P < 0.05, ***P < 0.001. HU, Habb-e-Ustukhuddus.

exhibited a significant 1.7 fold and 1.4 fold (P < 0.05) increase in the specific activity of GST at lower and higher doses, respectively (Figure 9L). Doxorubicin treatment similar to HU showed an increase in the specific activity of cyt P450R and GST from the basal level indicating its potential metabolization in the liver of mice.

Discussion

The central findings in the present study are: (a) a herbal formulation, Habb-e-Ustukhuddus showed novel anticancer activity against human epithelial cancer cells, (b) inhibited cell proliferation and survival, (c) increased sub-G1 phase cell population, (d) induced apoptosis involving dissipation of mitochondrial membrane potential and a strong increase in bax to bcl-2 ratio, (e) inhibited invasion and migration of cancer cells with a strong increase in E-cadherin to vimentin ratio, (f) showed the presence of bioactive compounds including flavonoids, and (g) its oral administration did not show any toxicity in mice.

Modern medicine finds inflammation an integral part

of tumor growth and promotion whereas the Unani system of medicine considers cancer as the disease of black bile humor (Hanahan and Weinberg, 2011; Naaz 2017). The herbal ingredients in the formulation of HU are well documented for their anti-inflammatory properties and known to be expellant of black bile (Ministry of Health and Family Welfare, 1983; Kalam et al., 2021). However, there is no scientific study done so far to explore the anticancer potential of HU. Therefore, for the first time, we studied the anticancer efficacy and associated mechanisms of HU on various epithelial cancer cells.

Our findings suggested that HU strongly inhibited the cell proliferation and cell viability of lung and breast cancer cells, which was accompanied by an increase in the population of dead cells. Cell proliferation and survival are regulated by balancing the cell cycle progression (Singh et al., 2021). HU treatment showing the increase in the sub-G1 phase population of cancer cells and retarded cell cycle progression might have led to the decrease in cell survival and cell number. The sub-G1 population is an indication of apoptosis induction in cells, hence, we further investigated the associated mechanisms of HU-caused
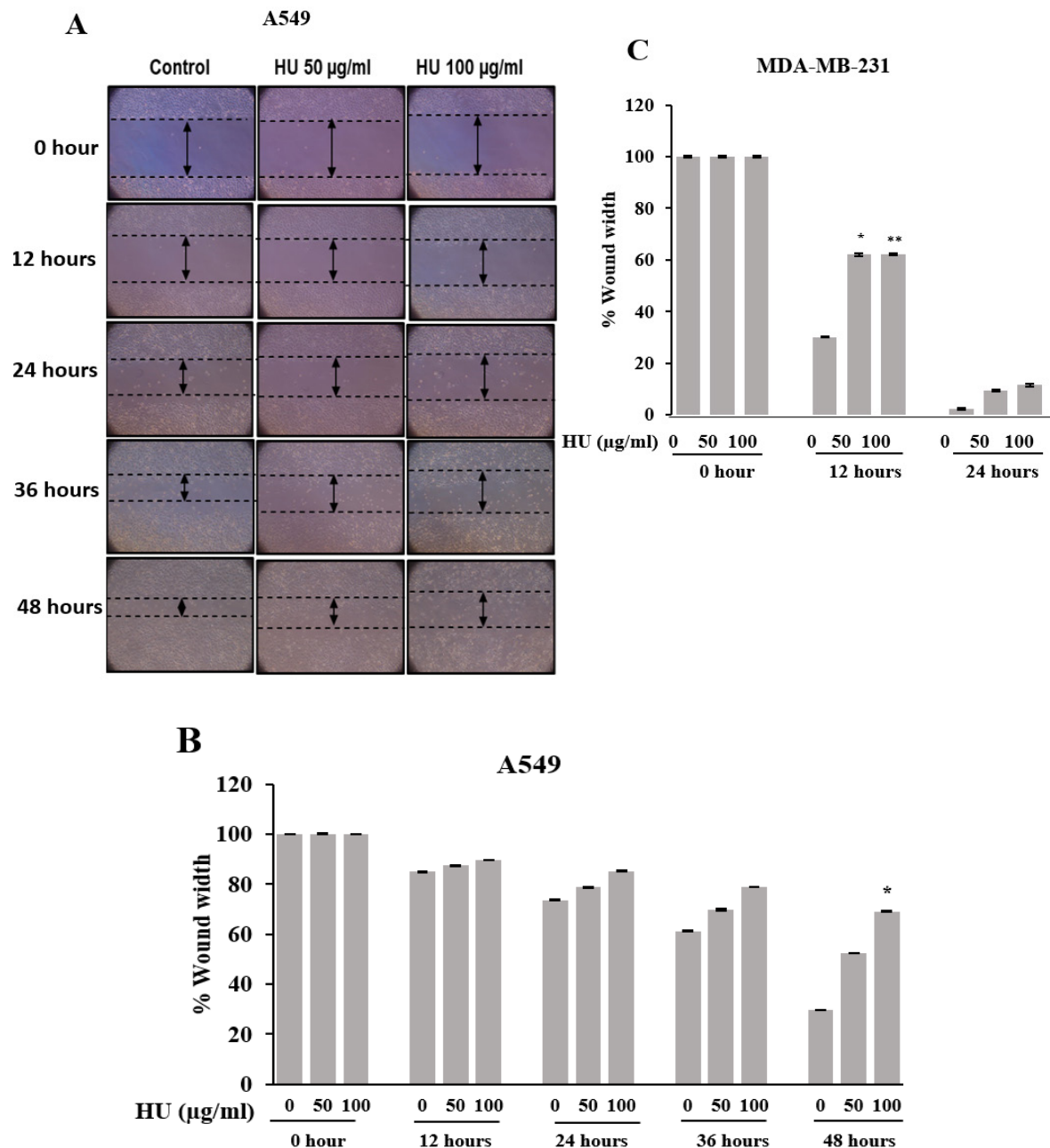
Figure 6. Effects of HU on Wound Closure of A549 and MDA-MB-231 Cells. (A) Representative image of A549 cell migration in response to HU treatment in wound healing assay which was performed in a 6-well culture plate. Images were taken at different time points at 100X magnifications. (B) Bar graphs represent the quantitative analysis of wound width in A549 cells and (C) MDA-MB-231 cells treated with HU. Data are shown as mean ± s.e.m. of three independent wells. Bars, s.e.m, *P < 0.05, **P < 0.01. HU, Habb-e-Ustukhuddus.

decrease in cancer cell survival. Depolarization of the mitochondrial membrane is an early sign of mitochondria-mediated apoptosis, which can be detected via flow cytometry using a JC-1 probe (Liang et al., 2017). With the treatment of HU, the mitochondrial membrane potential of cancer cells was depolarized. Mitochondrial membrane permeability is regulated by the Bcl-2 family of proteins during apoptosis (Lucken-Ardjomande and Martinou, 2005; Tan et al., 2006). We found that HU decreased the expression of Bcl-2 protein, increased the level of Bax, and thus, an overall elevated Bax/Bcl-2 ratio was observed. These changes in Bax to Bcl-2 ratio

are known to associated with the loss of mitochondrial membrane potential and release of cytochrome c in the cytosol, which further activates the caspases to induce apoptosis (Würstle et al., 2012; Kumar et al., 2019). Thus, our findings suggest that HU has a strong apoptotic effect on A549 lung cancer cells which is mediated through the activation of mitochondrial pathways.

Solid tumors can become more aggressive by epithelial-mesenchymal transitions (EMT), which enhances the invasiveness and metastatic activity of cancer cells (Derynck and Weinberg, 2019; Ribatti et al., 2020). Hence, we studied the effect of HU on EMT and found
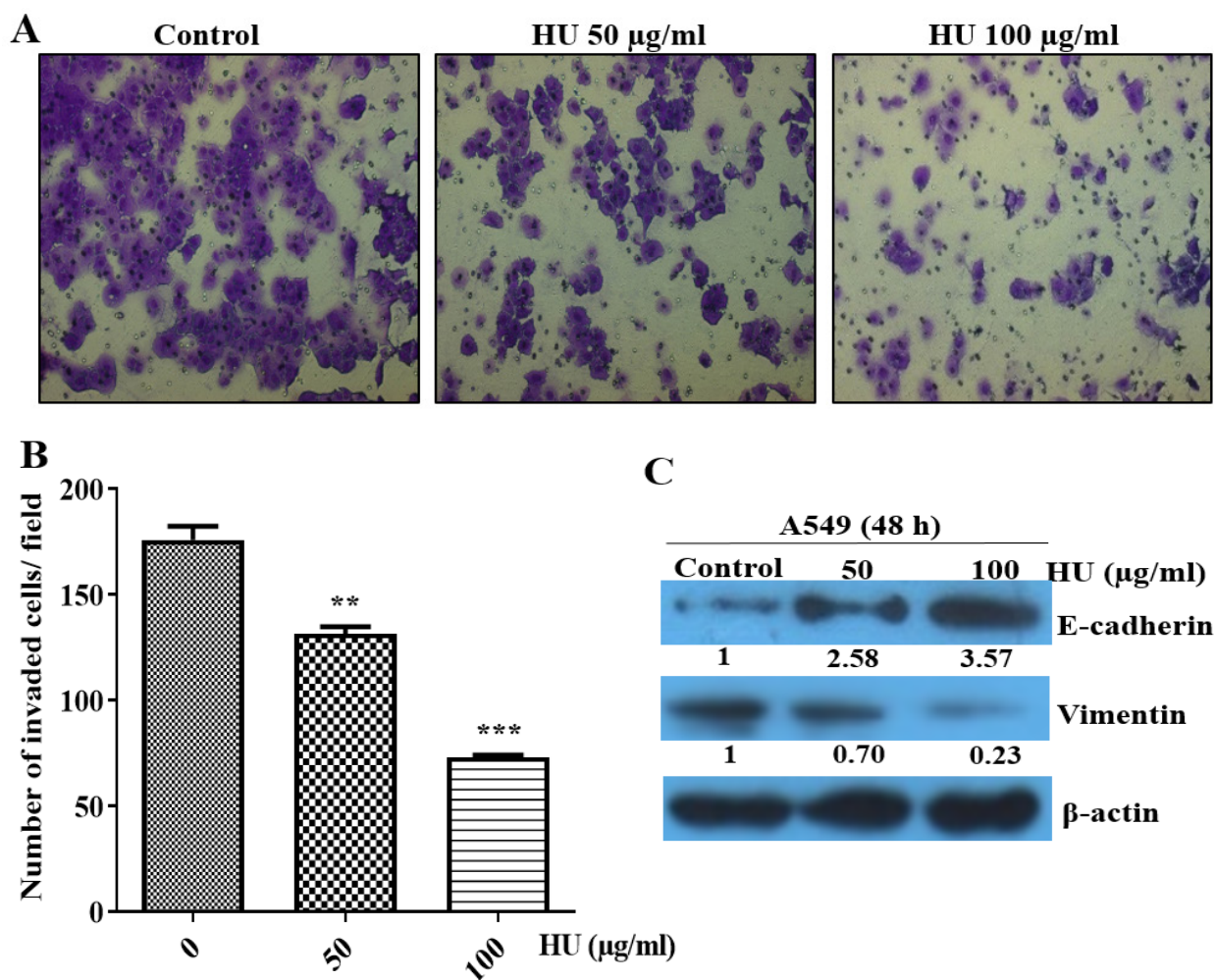
A

B

C

Figure 7. Effects of HU on Invasion Potential of A549 Cells. (A) Representative image of transwell invasion assay after treatment of cells with HU. (B) The bar graph represents the quantitative data of invaded cells/ field in A549 cells. Data are shown as mean ± s.e.m. of three independent wells. (C) Expression of the EMT markers, E-cadherin, and vimentin proteins from A549 cells, where β- actin was used as a loading control. Densitometry was performed using ImageJ software to determine the fold change of the proteins. Bars, s.e.m, **$P < 0.01$, ***$P < 0.001$. HU, Habb-e-Ustukhuddus.

that HU strongly inhibited the migration and invasion potential of lung and breast cancer cells at non-cytotoxic doses. During EMT, cells lose the adherents junction and downregulate the epithelial marker such as E-cadherin, and gain the invasive phenotype by upregulating mesenchymal markers such as vimentin (Ribatti et al., 2020). Consistent with this fact, HU increased the epithelial marker E-cadherin and decreased the mesenchymal marker vimentin, indicating the anti-metastatic effect of HU on cancer cells.

We did chemical profiling of the HU formulation to evaluate its phytochemical contents. GC-MS chromatogram obtained for the methanolic extract of HU showed the common presence of fatty acid, hexadecanoic acids, which possess antibacterial, antifungal (Chandrasekaran et al., 2011), anti-inflammatory (Aparna et al., 2012), antioxidant (Abubakar and Majinda, 2016), and antiandrogenic activities (Kumar et al., 2010). Another commonly present compound was 9,12-Octadecadienoyl chloride, which is reported for its cancer preventive effect along with hepatoprotective, hypocholesterolemic, antiandrogenic, antieczemic, and antihistaminic activities (Vijayabaskar

and Elango, 2018). HPLC chromatogram showed the presence of various known anticancer compounds in the methanolic extract of HU. Epicatechin, a polyphenol present in the highest amount in HU is reported to exhibit anti-proliferative, anti-angiogenic, antioxidant, and apoptotic effects against cancer cells (Shay et al., 2015; Abdulkhaleq et al., 2017). The other polyphenol, resveratrol detected in the formulation is under clinical trial for its anticancer activity (Varoni et al., 2016). Gallic acid, an endogenous plant polyphenol was present in HU and known to modulate the genes associated with cell cycle, apoptosis, angiogenesis, and apoptosis in cancer cells (Verma et al., 2013). The other detected bioactive compounds, such as vanillin (Bezerra et al., 2016), acetylsalicylic acid (Ausina et al., 2020), salicin (Sabaa et al., 2017), and epicatechin gallate (Min and Kwon, 2014) are reported to exhibit anticancer activities. Therefore, the chemical profile analysis of the HU Unani formulation helped us to understand the strong extraction capacity of methanol and the anticancer effects of the extract on lung and breast epithelial cancers in our study.

To further evaluate the chemopreventive potential of

A

GC-MS analysis of HU with representing the various components with retention time and % area		
Reten-tion time (min)	Area (%)	Name of compound
9.604	3.18	1,5-anhydro-6-deoxyhexo-2,3-diulose
10.937	11.30	5- Hydroxymethylfurfural
11.889	4.63	Furan-2-carbonsaeure, 3-methyl-, trimethylsilylester
12.552	17.02	Phenol, 2-methoxy-4-(2- propenyl)- $$ 4-allyl-2-methoxy-phenol $$ 1,3,4-eugenol $$ 1-(2-propenyl)-4-h
16.167	4.48	Cyclopentaneacetic acid, 3-oxo-2-(2-pentenyl)-, methyl ester, [1.alpha.,2.alpha.(Z)]- $$ Methyl (3-oxo-2-[(2Z)-2-pentenyl]cyclopentyl
16.402	2.29	5-Azulenemethanol
19.136	2.90	Hexadecanoic acid, methyl ester $$ Palmitic acid
19.549	3.04	n-Hexadecanoic acid
21.270	8.38	9,12-Octadecadienoyl chloride
25.425	2.95	10-Methyldodec-2-en-4-olide

B

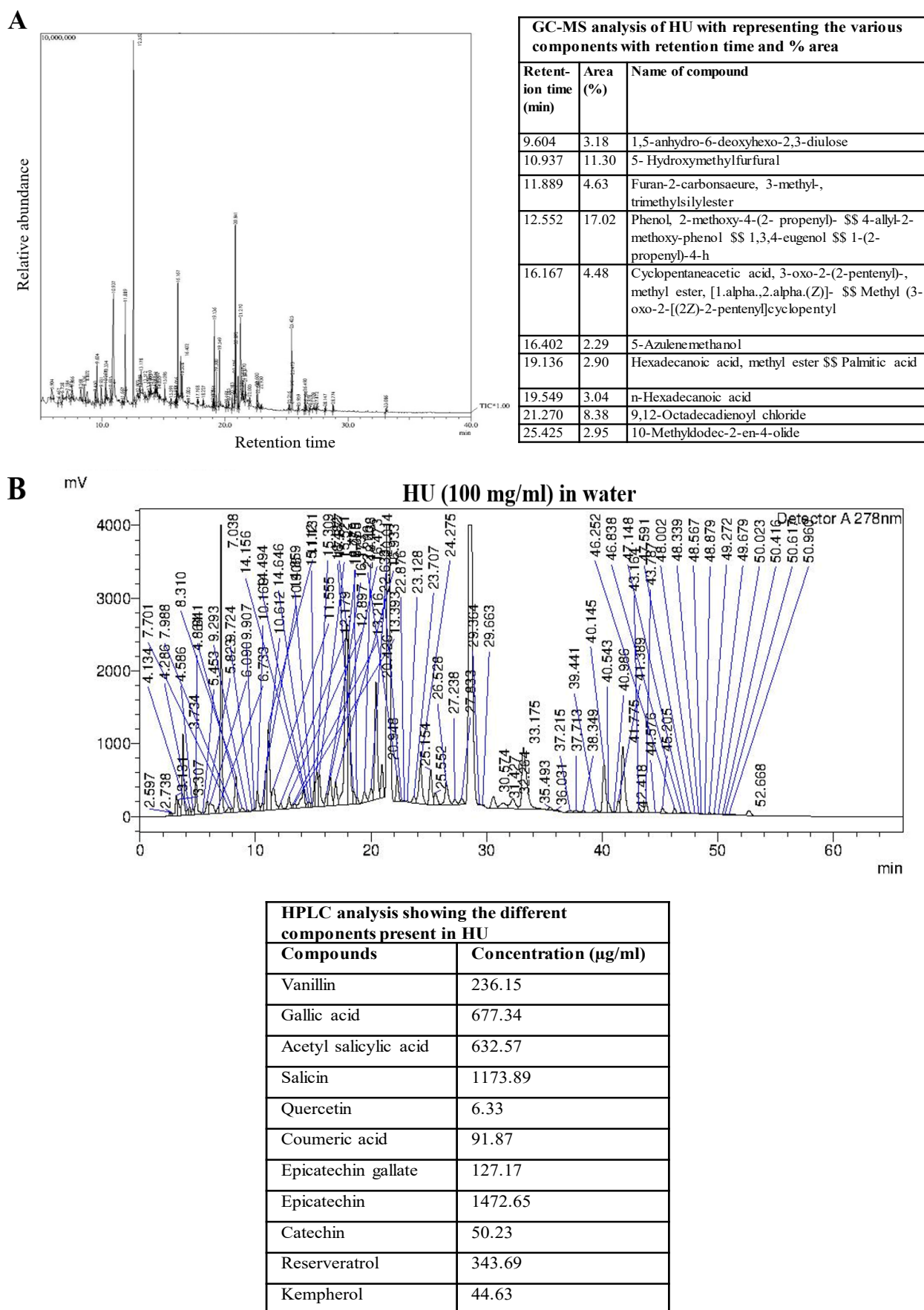| HPLC analysis showing the different components present in HU	
Compounds	Concentration (µg/ml)
Vanillin	236.15
Gallic acid	677.34
Acetyl salicylic acid	632.57
Salicin	1173.89
Quercetin	6.33
Coumeric acid	91.87
Epicatechin gallate	127.17
Epicatechin	1472.65
Catechin	50.23
Reserveratrol	343.69
Kempherol	44.63

Figure 8. Phytochemical Analysis of Methanolic Extract of HU by GC-MS and HPLC. GC-MS analysis of the methanolic extract of HU was performed. (A) GC-MS chromatogram (left panel) and the right panel representing the presence of various components with retention time and percent area are shown. Only the ten most abundant compounds are shown. (B) HPLC analysis of compounds present in methanolic extract of HU. HU extract was run through HPLC as described in the materials and methods. The presence of different components of HU was quantified by running standard compounds shown in the panel below the chromatogram.
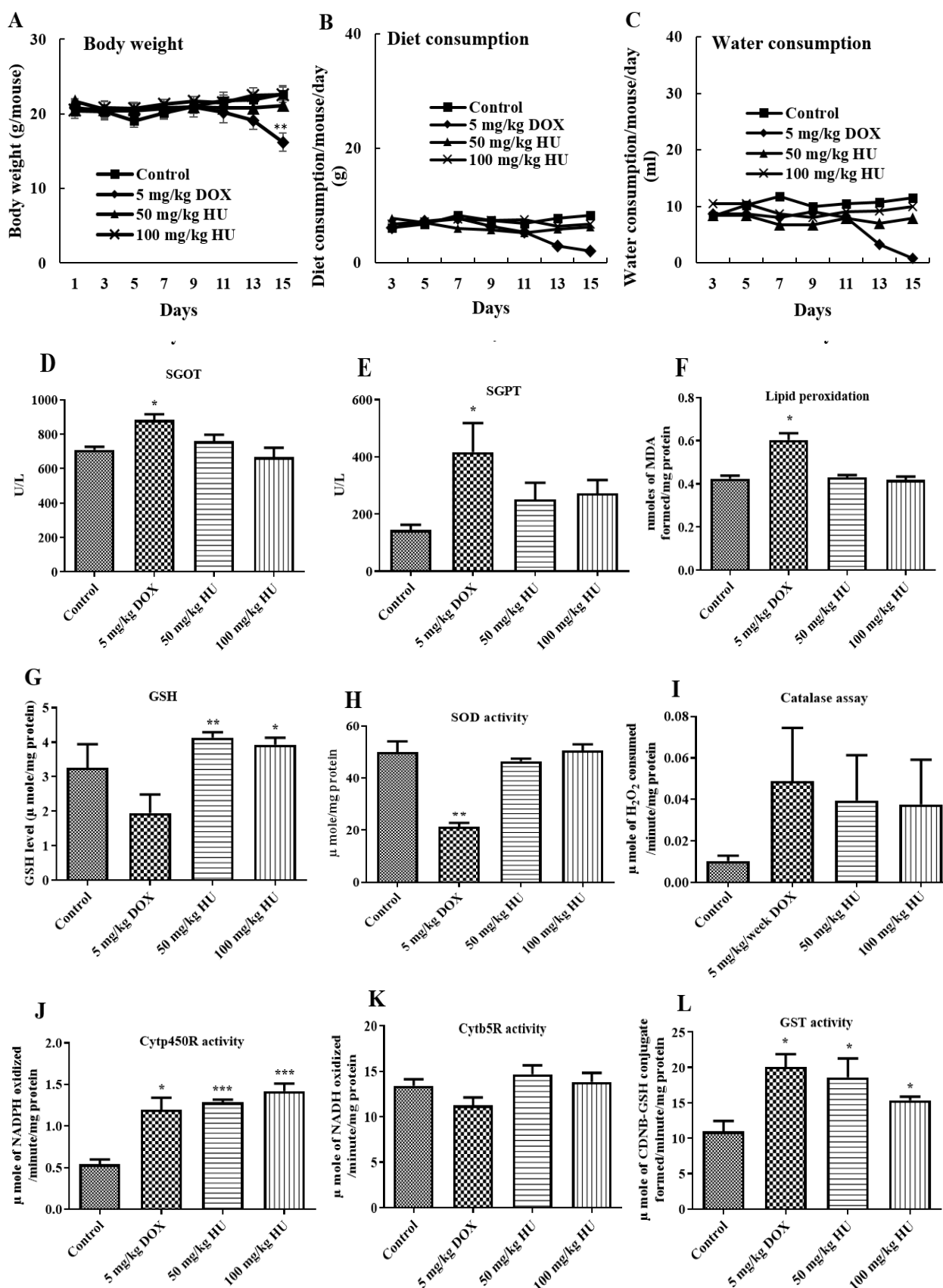
Figure 9. Effects of Oral HU on Toxicity Parameters in Mice. Male C57BL/6 mice were fed with HU at 50 and 100 mg/kg body weight of mouse for two weeks. (A) body weight, (B) diet, and (C) water consumption were recorded on every alternate day. (D-F) The toxic effect of HU on mice was measured by analysing SGOT, SGPT, and LPO activities. (G-I) The antioxidant effect of HU on mice's liver was measured by GSH content, SOD, and catalase activities. (J-L) Modulatory effects of HU on specific activities of hepatic enzymes Phase I drug-metabolizing enzymes cyt P450 reductase and cyt b5 reductase and phase II metabolic enzyme GST. Doxorubicin (5 mg/kg body weight of mouse) was used as a positive control. Values are expressed as mean ± s.e.m of six animals. Bars, s.e.m, *P < 0.05, **P < 0.01, ***P < 0.001.

HU, we examined its effect on the inducibility of enzymes associated with the metabolism of drugs and xenobiotics using animal models, and antioxidant status. Doxorubicin was used as a positive (toxic) control to authenticate the assay protocol since it is reported to induce a strong inflammatory response in male C57BL/6 mice, which was used in the study (Grant et al., 2020). There were no adverse health effects observed on animals at the given doses of HU (50 and 100 mg/kg body weight of the mouse, daily for 15 days). There was no indication of damage to the liver as SGOT, SGPT, and MDA formation remained unaltered after HU treatment. A decrease in the glutathione and activity of SOD by doxorubicin indicated oxidative damage to the liver, whereas, HU increased the glutathione level and thus antioxidant function in the liver of mice. Cytochrome P450 enzyme system, consisting of phase I and phase II enzymes, play key role in the metabolism, activation/ inactivation, detoxification, and elimination of drugs or xenobiotic compounds (McDonnell and Dang, 2013; Stavropoulou et al., 2018). Phase I metabolic enzymes convert the toxic agents into hydrophilic metabolites, and phase II enzymes use these metabolites as a substrate and convert them into water soluble products and facilitate their easy elimination from the body (Singh et al., 2000; Nauman et al., 2018). The increase in cytochrome P450 system and GST activities by HU showed its chemopreventive potential for the metabolization of xenobiotic compounds.

Overall, for the first time, this study identified the anticancer potential of HU against lung and breast epithelial cancer cells along with their underlined biological and molecular alterations. HU mediated growth inhibition by arresting the cancer cells in the sub-G1 phase and inducing mitochondria-mediated apoptotic cell death. Further, it inhibited the migration and invasion of cancer cells. HU also possesses chemopreventive potential without causing any hepatotoxicity or toxicity in mice, and thus it has a potential for cancer prevention and therapeutics which can be strengthened by further investigations.

Author Contribution Statement

R.P.S. designed the experiments and provided the intellectual input. R.P., and M.A. performed the experiments. R.P.S., Y.S., R.P., and M.A. wrote and edited the manuscript. All authors read and approved the final manuscript.

Acknowledgements

Ethical approval
The use of mice in this study was approved by Institutional Animal Ethics Committee (IAEC) of JNU and animal experiment was conducted at CLAR facility of JNU.

Data availability
Data sharing is applicable upon request by contacting the corresponding author.

The manuscript follows the MIRDA standard reporting recommendation (Ahmad, et al, 2022)

Conflict of interest
The authors declare no potential conflict of interest.

References

Abdulkhaleq LA, Assi MA, Noor MHM, et al (2017). Therapeutic uses of epicatechin in diabetes and cancer. *Vet World*, **10**, 869–72.

Abubakar MN, Majinda RRT (2016). GC-MS Analysis and Preliminary Antimicrobial Activity of Albizia adianthifolia (Schumach) and Pterocarpus angolensis (DC). *Medicines*, **3**, 3.

Aebi H. Catalase in vitro (1984). *Methods Enzymol*, **105**, 121–6.

Ahmad R, Riaz M, Aldholmi M, et al (2022). Development of a Critical Appraisal Tool (AIMRDA) for the Peer-Review of Studies Assessing the Anticancer Activity of Natural Products: A Step towards Reproducibility. *Asian Pac J Cancer Prev*, **22**, 3735-40.

Alam A, Ahmed S, Alam T, Azeez A (2013). Cancer (Sartan) and its management in Unani (Greco-Arab) system of medicine. *Int J Pharmamedix India*, **1**, 612–30.

Aparna V, Dileep KV, Mandal PK, et al (2012). Anti-inflammatory property of n-hexadecanoic acid: structural evidence and kinetic assessment. *Chem Biol Drug Des*, **80**, 434–9.

Aslam M, Bano H, Vohora SB (1981). Sartan (cancer) and its treatment in Unani Medicine. *Am J Chin Med*, **9**, 95–107.

Ausina P, Branco JR, Demaria TM, et al (2020). Acetylsalicylic acid and salicylic acid present anticancer properties against melanoma by promoting nitric oxide-dependent endoplasmic reticulum stress and apoptosis. *Sci Rep*, **10**, 19617.

Benetou V, Lagiou A, Lagiou P (2015). Chemoprevention of cancer: current evidence and future prospects. F1000Research, 4 (F1000 Faculty Rev):916.

Bezerra DP, Soares AKN, de Sousa DP (2016). Overview of the Role of Vanillin on Redox Status and Cancer Development. *Oxid Med Cell Longev*, **2016**, 9734816.

Buyel JF (2018). Plants as sources of natural and recombinant anti-cancer agents. *Biotechnol Adv*, **36**, 506–20.

Chandrasekaran M, Senthilkumar A, Venkatesalu V (2011). Antibacterial and antifungal efficacy of fatty acid methyl esters from the leaves of Sesuvium portulacastrum L. *Eur Rev Med Pharmacol Sci*, **15**, 775–80.

Derynck R, Weinberg RA (2019). EMT and Cancer: more than meets the eye. *Dev Cell*, **49**, 313–6.

Fernie AR, Trethewey RN, Krotzky AJ, Willmitzer L (2004). Metabolite profiling: from diagnostics to systems biology. *Nat Rev Mol Cell Biol*, **5**, 763–9.

Grant MKO, Abdelgawad IY, Lewis CA, Zordoky BN (2020). Sexual Dimorphism in Doxorubicin-induced Systemic Inflammation: Implications for Hepatic Cytochrome P450 Regulation. *Int J Mol Sci*, **21**, 1279.

Reenu Punia et al

Habig WH, Pabst MJ, Jakoby WB (1974). Glutathione S-transferases. The first enzymatic step in mercapturic acid formation. *J Biol Chem*, **249**, 7130–9.

Hanahan D, Weinberg RA (2011). Hallmarks of cancer: the next generation. *Cell*, **144**, 646–74.

Kalam MA, Husain Z, Haseeb A, et al (2021). Ustukhuddus (Lavandula stoechas L.): A boon for the management of neuropsychiatric disorders in perspective of Unani medicine-a review. *Acta Sci Pharm Sci*, **5**, 2-9.

Kell DB, Brown M, Davey HM, et al (2005). Metabolic footprinting and systems biology: the medium is the message. *Nat Rev Microbiol*, **3**, 557–65.

Kumar K, Sabarwal A, Singh RP (2019). Mancozeb selectively induces mitochondrial-mediated apoptosis in human gastric carcinoma cells through ROS generation. *Mitochondrion*, **48**, 1–10.

Kumar PP, Kumaravel S, Lalitha C (2017). Screening of antioxidant activity, total phenolics and GC-MS study of Vitex negundo. *Afr J Biochem Res Acad J*, **4**, 191–5.

Liang W, Cui J, Zhang K, et al (2017). Shikonin induces ROS-based mitochondria-mediated apoptosis in colon cancer. *Oncotarget*, **8**, 109094–106.

Lucken-Ardjomande S, Martinou J-C (2005). Regulation of Bcl-2 proteins and of the permeability of the outer mitochondrial membrane. *C R Biol*, **328**, 616–31.

Marklund S, Marklund G (1974). Involvement of the Superoxide Anion Radical in the Autoxidation of Pyrogallol and a Convenient Assay for Superoxide Dismutase. *Eur J Biochem*, **47**, 69–74.

McDonnell AM, Dang CH (2013). Basic Review of the Cytochrome P450 System. *J Adv Pract Oncol Harborside Press*, **4**, 263.

Miller KD, Siegel RL, Lin CC, et al (2016). Cancer treatment and survivorship statistics, 2016. *CA Cancer J Clin*, **66**, 271–89.

Min K, Kwon TK (2014). Anticancer effects and molecular mechanisms of epigallocatechin-3-gallate. *Integr Med Res*, **3**, 16–24.

Ministry of Health & Family Welfare (1983). National Formulary of Unani Medicine, Part 1, Volume 1. Department of Ayurveda, Yoga & Naturopathy, Unani, Siddha and Homoeopathy (AYUSH), Ministry of Health & Family Welfare, Government of India.

Naaz F (2017). Integration of Unani medicine in cancer management. *World J Pharm Res*, **6**, 450–61.

Nag M, Kar A, Chanda J, Mukherjee PK (2020). RP-HPLC analysis of methanol extract of Viscum articulatum. *J Ayurveda Integr Med*, **11**, 277–80.

Nair PKR, Melnick SJ, Wnuk SF, et al (2009). Isolation and characterization of an anticancer catechol compound from Semecarpus anacardium. *J Ethnopharmacol*, **122**, 450–6.

Nauman M, Kale RK, Singh RP (2018). Polyphenols of Salix aegyptiaca modulate the activities of drug metabolizing and antioxidant enzymes, and level of lipid peroxidation. *BMC Complement Altern Med*, **18**, 81.

Palmieri A, Scapoli L, Iapichino A, et al (2019). Berberine and Tinospora cordifolia exert a potential anticancer effect on colon cancer cells by acting on specific pathways. *Int J Immunopathol Pharmacol*, **33**, 2058738419855567.

Punia R, Raina K, Agarwal R, Singh RP (2017). Acacetin enhances the therapeutic efficacy of doxorubicin in non-small-cell lung carcinoma cells. *PLoS One*, **12**, e0182870.

Rai M, Jogee PS, Agarkar G, dos Santos CA (2016). Anticancer activities of Withania somnifera: Current research, formulations, and future perspectives. *Pharm Biol*, **54**, 189–97.

Rajput M, Singh R, Singh N, Singh RP (2021). EGFR-mediated Rad51 expression potentiates intrinsic resistance in prostate cancer via EMT and DNA repair pathways. *Life Sci*, **286**, 120031.

Ravi Shankara BE, Ramachandra YL, Rajan SS, et al (2016). Evaluating the Anticancer Potential of Ethanolic Gall Extract of Terminalia chebula (Gaertn.) Retz. (Combretaceae). *Pharmacogn Res*, **8**, 209–12.

Ribatti D, Tamma R, Annese T (2020). Epithelial-Mesenchymal Transition in Cancer: A Historical Overview. *Transl Oncol*, **13**, 100773.

Sabaa M, ELFayoumi HM, Elshazly S, Youns M, Barakat W (2017). Anticancer activity of salicin and fenofibrate. *Naunyn Schmiedebergs Arch Pharmacol*, **390**, 1061–71.

Sabarwal A, Agarwal R, Singh RP (2017). Fisetin inhibits cellular proliferation and induces mitochondria-dependent apoptosis in human gastric cancer cells. *Mol Carcinog*, **56**, 499–514.

Sengupta M, Sharma GD, Chakraborty B (2011). Hepatoprotective and immunomodulatory properties of aqueous extract of Curcuma longa in carbon tetra chloride intoxicated Swiss albino mice. *Asian Pac J Trop Biomed*, **1**, 193–9.

Shafi G, Hasan TN, Syed NA, et al (2012). Artemisia absinthium (AA): a novel potential complementary and alternative medicine for breast cancer. *Mol Biol Rep*, **39**, 7373–9.

Shay J, Elbaz HA, Lee I, et al (2015). Molecular mechanisms and therapeutic effects of (−)-epicatechin and other polyphenols in cancer, inflammation, diabetes, and neurodegeneration. Oxid Med Cell Longev. *Hindawi*, **2015**, e181260.

Shyanti RK, Sehrawat A, Singh SV, Mishra JPN, Singh RP (2017). Zerumbone modulates CD1d expression and lipid antigen presentation pathway in breast cancer cells. *Toxicol Vitro Int J Publ Assoc BIBRA*, **44**, 74–84.

Singh N, Nambiar D, Kale RK, Singh RP (2013). Usnic acid inhibits growth and induces cell cycle arrest and apoptosis in human lung carcinoma a549 cells. *Nutr Cancer Routledge*, **65**, 36–43.

Singh R, Rajput M, Singh RP (2021). Simulated microgravity triggers DNA damage and mitochondria-mediated apoptosis through ROS generation in human promyelocytic leukemic cells. *Mitochondrion*, **61**, 114–24.

Singh RP, Banerjee S, Rao AR (2000). Effect of Aegle marmelos on biotransformation enzyme systems and protection against free-radical-mediated damage in mice. *J Pharm Pharmacol*, **52**, 991–1000.

Sivasankarapillai VS, Madhu Kumar Nair R, Rahdar A, et al (2020). Overview of the anticancer activity of withaferin A, an active constituent of the Indian ginseng withania somnifera. *Environ Sci Pollut Res*, **27**, 26025–35.

Soni D, Grover A (2019). "Picrosides" from Picrorhiza kurroa as potential anti-carcinogenic agents. *Biomed Pharmacother*, **109**, 1680–7.

Stavropoulou E, Pircalabioru GG, Bezirtzoglou E (2018). The Role of Cytochromes P450 in Infection. *Front Immunol*, **9**, 89.

Sung H, Ferlay J, Siegel RL, et al (2021). Global Cancer Statistics 2020: GLOBOCAN estimates of incidence and mortality worldwide for 36 cancers in 185 countries. *CA Cancer J Clin*, **71**, 209–49.

Suresh V, Sruthi V, Padmaja B, Asha VV (2011). In vitro anti-inflammatory and anti-cancer activities of Cuscuta reflexa Roxb. *J Ethnopharmacol*, **134**, 872–7.

Tan C, Dlugosz PJ, Peng J, et al (2006). Auto-activation of the apoptosis protein Bax increases mitochondrial membrane permeability and is inhibited by Bcl-2. *J Biol Chem*, **281**, 14764–75.

Uddin Q, Amanullah, Siddiqui KM, Rahman RU (2015). Unani medicine for cancer care: an evidence-based review. *Int J Ayurvedic Herb Med*, **5**, 1811–25.

Varoni EM, Lo Faro AF, Sharifi-Rad J, Iriti M (2016). Anticancer

molecular mechanisms of resveratrol. *Front Nutr*, **3**, 8.

Varshney R, Kale RK (1990). Effects of calmodulin antagonists on radiation-induced lipid peroxidation in microsomes. Int *J Radiat Biol*, **58**, 733–43.

Verma S, Singh A, Mishra A (2013). Gallic acid: Molecular rival of cancer. *Environ Toxicol Pharmacol*, **35**, 473–85.

Vijayabaskar G, Elango V (2018). Determination of phytocompounds in Withania somnifera and Smilax china using GC-MS technique. *J Pharmacogn Phytochem*, **7**, 554–7.

Wurstle ML, Laussmann MA, Rehm M (2012). The central role of initiator caspase-9 in apoptosis signal transduction and the regulation of its activation and activity on the apoptosome. *Exp Cell Res*, **318**, 1213–20.

Zhao T, Sun Q, Marques M, Witcher M (2015). Anticancer properties of Phyllanthus emblica (Indian Gooseberry). *Oxid Med Cell Longev*, **2015**, 950890.